ELSEVIER

Journal of Alloys and Compounds 408–412 (2006) 66–70

Journal of ALLOYS AND COMPOUNDS

www.elsevier.com/locate/jallcom

Electrochemically produced divalent neodymium in chloride melt

Hajimu Yamana[a,*], Byung Gi Park[b], Osamu Shirai[a], Toshiyuki Fujii[a], Akihiro Uehara[a], Hirotake Moriyama[c]

[a] *Research Reactor Institute, Kyoto University, 2-1010, Asashiro Nishi, Kumatori-cho, Sennan-gun, Osaka 590-0494, Japan*
[b] *FNC Technology Co. Ltd., SNU Research Innovation Cent., Gwanak-gu, Seoul 151-818, Republic of Korea*
[c] *Department of Nuclear Engineering, Graduate School of Kyoto University, Yoshida-honmachi, Sakyo-ku, Kyoto 606-8501, Japan*

Abstract

Production of Nd^{2+} by cathodic electrolysis of $NdCl_3$ dissolved in molten LiCl–KCl was tested at 773 K. Cyclic voltammetry and differential pulse voltammetry were adopted for the determination of the formal redox potential between Nd^{3+} and its divalent or metallic states. UV–visible absorption spectrophotometry was carried out at the vicinity of the cathode during the simultaneous electrolysis at −1.9 V versus Ag/Ag^+. During the electrolysis, growth of a new broad absorption band ranging from 450 to 580 nm was observed and this was attributed to the absorption by the chloride complex of Nd^{2+} formed by the electrochemical reduction of $NdCl_3$. Black precipitate formed in the melt as a result of the constant potential electrolysis over long-period was analyzed by EPMA and ICP-AES and they were confirmed to be fine particles of Nd. The results were discussed in relation to the disproportionation of Nd^{2+} and reaction with quartz vessel.

Keywords: Neodymium; Divalent neodymium; Absorption spectrophotometry; Molten chloride; Voltammetry

1. Introduction

The chemical characteristics of lanthanides in chloride melts merit further investigation for enhancing the chemical basis of lanthanides in molten salts and for developing techniques for lanthanide refining. One of the particular interests in relation to the performance of the electrolytic refining of lanthanides in molten salts is the formation of lanthanide's less-common valence states [1–3]. Lanthanides having less energetic difference between electron configurations $4f^{n-1}6s^25d^1$ and $4f^n6s^25d^0$ are likely to form stable or meta-stable divalent state [4], especially in non-oxidizing conditions like molten chlorides. Nd is one of the lanthanides that have divalent compounds and it has been investigated in some particular organic solvents or solid matrix [5–7]. However, the formation of Nd^{2+} in LiCl–KCl eutectic melt has not been sufficiently investigated. The purpose of this study is to find the condition of the formation of Nd^{2+} by cathodic electrolysis of Nd^{3+} in molten LiCl–KCl and to examine the stability of produced Nd^{2+} in molten LiCl–KCl. A special focus is put on the disproportionation reaction and reaction with the vessel material of Nd^{2+}.

2. Experimental

2.1. Sample preparation

All the experiments were carried out in a glove box system filled with dry Ar continuously purified to remove oxygen and humidity. The content of impurity O_2 and H_2O in the inside atmosphere was continuously maintained less than 1 ppm. Anhydrous LiCl–KCl was purchased from APL Ltd. and used without further purification. Anhydrous NdCl3 purchased from APL Ltd. was used without further treatment for electrochemical analysis. Anhydrous $NdCl_3$, purchased from APL Ltd. and was used without further treatment for electrochemical analysis. Anhydrous $NdCl_3$ purchased from Kojundo Chemical Laboratory Co. Ltd. was used for spectrophotometric measurements.

---

* Corresponding author. Tel.: +81 724 51 2442; fax: +81 724 51 2634.
E-mail address: yamana@HL.rri.kyoto-u.ac.jp (H. Yamana).

0925-8388/$ – see front matter © 2005 Elsevier B.V. All rights reserved.
doi:10.1016/j.jallcom.2005.04.104

2.2. *Cyclic voltammetry and differential pulse voltammetry*

0.117 g of $NdCl_3$ was dissolved into 11.178 g of molten LiCl–KCl at 773 K. Test tubes of quartz of 13 mm inner diameter were used for the measurement. A 1.0 mm Ø molybdenum rod was used for working electrode and a graphite rod of the same diameter was used for counter electrode, both covered with alumina sheath. A reference electrode, Ag/LiCl–KCl–AgCl (1 mol%) contained in a PYREX glass membrane tube was used. Polarization measurement system HZ-3000 (Hokuto-denko Co. Ltd.) was used for the voltammetry measurements. All measurements were performed at 773 ± 5 K. The differential pulse voltammetry was performed on a pulse period of 0.1 s with the square pulse having 0.01 V amplitude and 0.05 s width.

2.3. *Absorption spectrophotometry under simultaneous electrolysis*

Absorption spectrophotometry under electrolysis was carried out using a transparent quartz cell illustrated in Fig. 1. The details of the absorption measurement system can be seen elsewhere [8]. The tungsten working electrode was deeply immersed into the solution so that the light passed through the vicinity of its surface. The very thin tip of the PYREX glass at the end of the counter electrode worked as an electroconductive separator for the anode cell. Three kinds of working electrode were tested: tungsten mesh electrode (mesh made of 0.03 mm Ø tungsten wire, 50 mesh/in.); tungsten coil electrode made of 0.6 mm Ø tungsten wire; U-shaped electrode made of 0.8 mm Ø tungsten rod. These three electrodes were designed to give higher electrode surface area in the light path, but not to screen the light so much. The temperature of the sample during the experiment was controlled to 773 K within $\pm 5^{\circ}$.

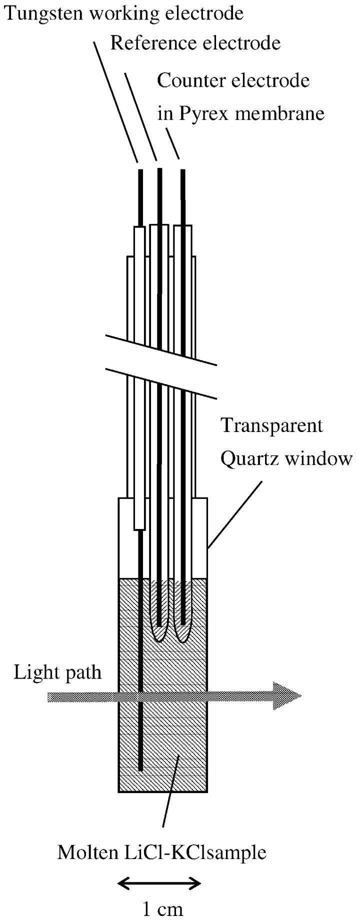

Fig. 1. Electrode arrangement for the spectrophotometry under simultaneous electrolysis.

2.4. *Long-period electrolysis followed by ICP-AES and EPMA analysis*

Using the same electrode arrangement to the voltammetry measurements, constant potential electrolysis of Nd^{3+} was performed using a quartz tube. The electrolysis was performed at −1.9 V versus Ag/Ag^{+}, which is the potential at which the reduction of Nd^{3+} to Nd^{2+} was expected to proceed. The melt was visually observed several times during the electrolysis and it was sampled after the end of the electrolysis, especially from the bottom of the cell. Qualitative element analysis was performed by EPMA for the frozen salt sample containing black precipitates, which had been formed during the electrolysis. The salt sample was once dissolved in water and the undissolved black precipitates were removed by filtration. The separated precipitates were completely dissolved in diluted hydrochloric acid and the amount of Nd was analyzed by ICP-AES. Powder X-ray diffraction pattern of the salt samples were taken by X-ray diffractometer.

3. Results and discussions

3.1. *Voltammetry measurement*

Fig. 2 shows the cyclic voltammogram of $NdCl_3$ in LiCl–KCl at 773. The potential was swept from natural potential, which is about −0.4 V versus Ag/Ag^{+}, toward negative direction and it had been reversed before the reduction of Li^{+} began. The reduction peak of $Nd^{3+} \rightarrow Nd^{0}$ is seen at about −2.1 V versus Ag/Ag^{+} and this is followed by an intensive oxidation peak. The peak potential of the major reduction current, which was taken at the scanning rate of 100 $mV\,s^{-1}$, was −2.062 V versus Ag/Ag^{+} for 773 K. A small growth of the reduction current can be seen in the region from −1.8 to −1.9 V versus Ag/Ag^{+} before the peak of $Nd^{3+} \rightarrow Nd^{0}$ grows, which can be assigned to the one-electron reduction of $Nd^{3+} \rightarrow Nd^{2+}$. The oxidation peak of Fig. 2 appears to consist of two components and this is different from the sharper oxidation peaks shown by other lanthanides having no divalent states. Fig. 3 shows the result of the differential pulse voltammetry. At scanning rate of 20 mVs^{-1}, $E_{1/2}$ of the small

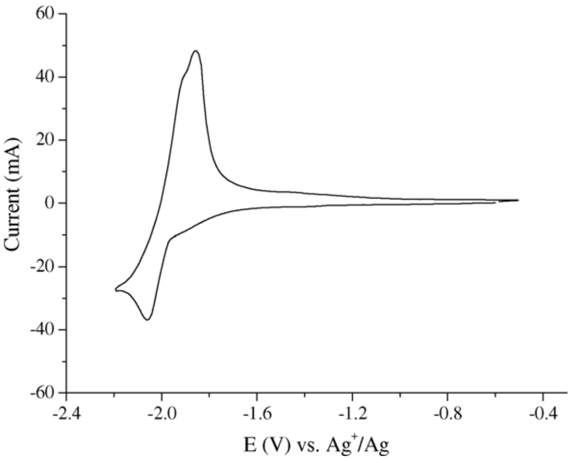

Fig. 2. Cyclic voltammogram of Nd^{3+} in LiCl–KCl at 773 K.

peak and major peak were found to be −1.89 and −2.01 V versus Ag/Ag^+, respectively. It was found that the small peak did not depend on the potential scanning rate so much, but the major peak showed a slight dependence. Taking into consideration that these dependences on the scanning rate were not large, especially at lower scanning rates, they were treated as reversible reactions for estimating their formal potentials. Formal potentials of the reaction $Nd^{3+} \rightarrow Nd^{2+}$ was estimated from the $E_{1/2}$ of differential pulse voltammetry using equation (1) [9], by adopting unity to the activity coefficient γ. That of $Nd^{3+} \rightarrow Nd^0$ was estimated from the E_p, peak potential of reduction current, of cyclic voltammetry using equation (2) [10], by adopting unity to the activity coefficient f_{ox}.

$$E_{1/2} = E^{o} + \frac{RT}{F} \ln\left(\frac{D_{2+}}{D_{3+}}\right)^{1/2} + \frac{RT}{F} \ln\frac{\gamma_{3+}}{\gamma_{2+}} + E_{ref} \tag{1}$$

$$E_p = E^{o} + \frac{0.153}{n} \log f_{ox}C_o - \frac{0.0568}{n} + E_{ref}, \quad \text{at } 773\,\text{K} \tag{2}$$

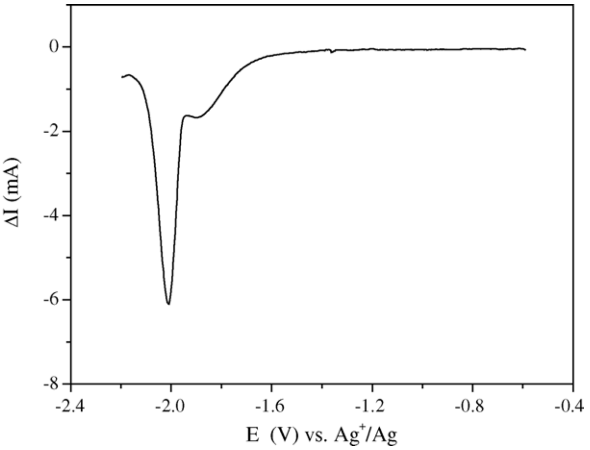

Fig. 3. Differential pulse voltammogram of Nd^{3+} in LiCl–KCl at 773 K.

Table 1
Results of the redox potential measurements

E^*(3–0) (V vs. Cl_2/Cl^-)	−3.25 ± 0.01
E^*(3–2) (V vs. Cl_2/Cl^-)	−3.178 ± 0.005
E^*(2–0) (V vs. Cl_2/Cl^-)	−3.286 ± 0.015
ΔG°_{dis} (kJ)	20.8 ± 3.2

In these equations, D is a diffusion coefficient of suffixed species, C_o the bulk concentration and E_{ref} is the potential of reference electrode which is 1.263 V for Ag/LiCl–KCl–AgCl (1 mol%). Though D_{2+} and D_{3+} of Nd are unclear, since it is considered that the ratio of D_{2+} and D_{3+} of lanthanides does not vary largely because of their monotonic trend of the ionic radius contraction along the series, D_{2+}/D_{3+} of similar lanthanide was adopted as an approximation. In this paper, D_{2+} and D_{3+} of Eu, which have been reported [9], were adopted for Nd. These approximations resulted in larger errors of the determined potentials. Derived formal potentials, E^*(3–2) and E^*(3–0), are summarized in Table 1. E^*(2–0) derived from other two was also shown in Table 1.

3.2. Spectrophotometry under simultaneous electrolysis

Before starting the electrolysis, the absorption spectrum was obtained for the $NdCl_3$ sample. The absorption spectrum of $NdCl_3$ is shown in Fig. 4(a), in which an intensive hypersensitive absorption peak of Nd^{3+} can be seen at 589 nm. Electrolysis was performed at a potential about −1.9 V versus Ag/Ag^+ by controlling the negative current to 1 or 2 mA. This

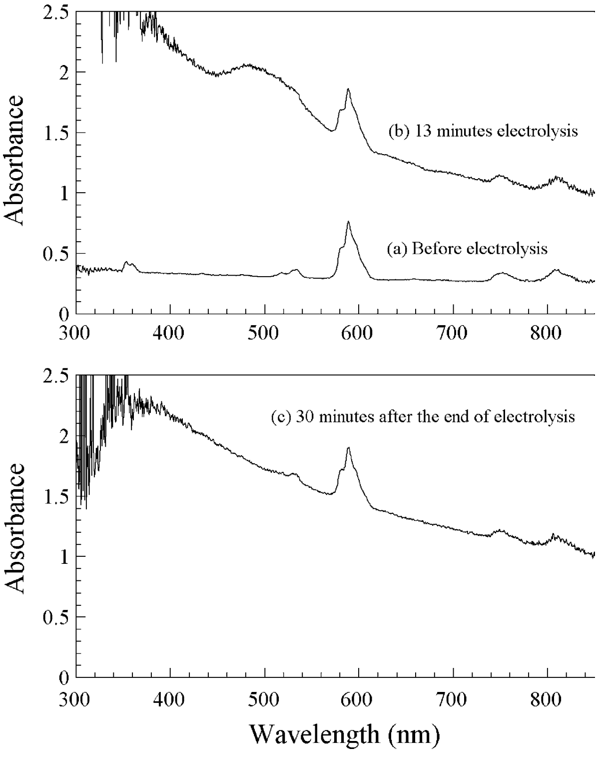

Fig. 4. UV–visible absorption spectrum of Nd^{3+} in LiCl–KCl under electrolysis.

potential was expected to allow the reaction $Nd^{3+} \rightarrow Nd^{2+}$, but not to allow the formation of Nd^0 by the reduction of Nd^{3+}. The absorption spectrum obtained about 13 min after the start of the electrolysis is shown in Fig. 4(b). Fig. 4(b) is a spectrum obtained by use of U-shaped rod electrode, but similar spectra were obtained for other two types of electrode. This spectrum is characterized by the appearance of a new broad absorption band in the region from 450 to 580 nm. As the time passed during the electrolysis, the spectrum gradually slanted. The inclination of the background line of the spectrum is possibly attributable to the increased light scattering or the slight change of the color of the silica window as a result of the electrolysis; it may be also due to a particular absorption by the product of the electrolysis. Fig. 4(c) indicates the spectrum obtained 30 min after the stop of the electrolysis. It should be emphasized that the broad absorption band in the region from 450 to 580 nm completely disappeared on the high inclined background within about 2 min after the electrolysis was stopped.

The absorption peak at 589 nm observed before the electrolysis can be assigned to the hypersensitive f–f transitions of Nd^{3+}[11] and it did not change during the electrolysis. The broad absorption band ranging from 450 to 580 nm grew only during the electrolysis and it quickly disappeared after stopping the electrolysis. By the literatures about absorption spectra of divalent iodides of Nd in tetrahydroflan (THF) [5] and in CaF_2 [7], it has been reported that Nd^{2+} in THF shows a broad absorption band ranging from 450 to 600 nm which consists of two peaks at 507 and 540 nm[5], and that Nd^{2+} in CaF_2 [7] shows a broad absorption band over the region from 520 to 640 nm showing a maximum at 590. Since the broad absorption band was observed under a particular negative potential that corresponds to the reduction $Nd^{3+} \rightarrow Nd^{2+}$ and since its wave length region agrees well with that observed for NdI_2 in THF and CaF_2, it should be considered that this broad absorption is of the electrochemically produced Nd^{2+} by the electrolysis in the melt. This assignment well agrees with the result by Terakado et al. [12]. In general, the electronic transitions, which give rise to the broad absorption bands of divalent lanthanides ion in various ligand fields are considered to be transitions between $4f^n$ and $4f^{n-1}5d^1$ electron configurations [13]. Therefore, it should be a transition between $4f^4$ and $4f^35d^1$ electron configurations of Nd^{2+} ion in LiCl–KCl. This should correspond to the transition from ^5I to ^4F d, which is about 20 kcm^{-1} in CaF_2 matrix [13]. In general, f–d transition, which is Laporte allowed, shows very intensive molar absorptivity than f–f transition, but the observed absorbance is as high as hypersensitive peak of 589 nm. This means that the average concentration of formed Nd^{2+} was quite low, suggesting that quite limited amount of Nd^{2+} was observed only in the vicinity of the cathode. The large inclination of the base line, which is considered to be partly attributable to the change of the light scattering or window conditions, may also be attributable to the intervalence charge transfer [13].

3.3. Long-period electrolysis

Electrolysis at −1.9 V versus Ag/Ag^+ was performed for about 2 h using the same electrode arrangement as the spectrophotometry measurement. By the visual observation during the electrolysis, it was found that the melt entirely became black at the mid time, but that it became clear as the electrolysis proceeded. At the end of the electrolysis, very black precipitate settled down to the bottom of the cell with very clear melt left in the upper part. The inside surface of the quartz cell became lightly black and partly light brown. After the end of the electrolysis, the bottom of the quartz tube became completely black and lost its glassy nature. The qualitative chemical analysis of the black precipitate by EPMA and ICP-AES showed that the major component of this precipitate was Nd. On the other hand, the XRD pattern of the salt sample, which contained a little amount of fine black particles, did not obviously show the diffraction patterns of Nd metal or Nd oxide.

3.4. Stability of electrochemically produced Nd^{2+}

The low observed absorbance and the rapid disappearance of this broad absorption within about 4 min after stopping the electrolysis, suggests the instability of the electrochemically produced Nd^{2+} in this system. The intensity of the broad absorption was approximately kept constant over the period later than about 10 min from the start of the electrolysis and this indicates that the generation and the disappearance of Nd^{2+} in the measured region were equilibrated during the electrolysis. According to the general understanding that the instability of divalent species with respect to its oxidation is in proportion to the instability with respect to the disproportionation [3], Nd^{2+} is likely to disproportionate into Nd^0 and Nd^{3+} by reaction (3),

$$3Nd^{2+}(\text{melt}) \rightarrow Nd^0 + 2Nd^{3+}(\text{melt}) \qquad (3)$$

where Nd^{3+}(melt) and Nd^{2+}(melt) means chloro-complex of these cations in the melt, $NdCl_6{}^{3-}$ and $NdCl_x{}^{(x-2)-}$, respectively. The standard Gibbs energy change of reaction (3), $\Delta G^\circ_{\text{dis}}$, can be given by

$$\Delta G^\circ_{\text{dis}} = 3F(E^*(3\text{–}2) - E^*(3\text{–}0)). \qquad (4)$$

With the use of the formal potentials listed in Table 1, $\Delta G^\circ_{\text{dis}} = 20.8 \pm 3.2$ kJ/mol is obtained for reaction (3) at 773 K. Due to this slightly positive value of $\Delta G^\circ_{\text{dis}}$, equilibrium (3) is likely to be sided to the left-side under the presence of the metal. However, under the continuous production of Nd^{2+} by the electrolysis, at the vicinity of the electrode surface, the local concentration of Nd^{2+} becomes high and leads to disproportionation into Nd^0 and Nd^{3+}. Aggregation and settling down of the metallic fines accelerate the disproportionation more. Nd^0 formed by reaction (3), as metallic fog, explains the dark color of the melt during the electrolysis and the settle down of the black precipitate to the bottom. Clear XRD patterns of metal or oxide of Nd in the salt sample were not observed, but this suggests that the Nd precipitates were not in a clear crystallographic condition. The usage of the quartz cell must have accelerated the loss of produced Nd^{2+} by the reaction with SiO_2. Nd^{2+}(melt) is so unstable with respect to re-oxidation that it reacts with the quartz window to form oxide or oxichloride of Nd^{3+} and the color change of inside wall of the quartz tube to light black or brown should be the evidence of the reduction of SiO_2 to SiO by Nd^{2+}. The bottom of the quartz cell encountered with large amount of black precipitates, of metallic Nd and it is considered to have reacted with Nd^0 to form Nd oxide or oxichloride and broke the glass surface.

4. Conclusions

By electrochemical measurements, the formal redox potentials of the reduction of Nd^{3+} to metal and Nd^{2+} in molten LiCl–KCl were determined. By means of UV–visible absorption spectrophotometry performed under simultaneous electrolysis of $NdCl_3$ in molten LiCl–KCl, a broad absorption band ranging from 450 to 580 nm was observed and this was attributed to the Nd^{2+} formed by electrochemical reduction. Analysis and visual observation of the melt during the electrolysis showed the formation of Nd precipitates and this was attributed to the result of the disproportionation reaction of Nd^{2+}.

Acknowledgments

Authors are indebted to Prof. Tsutomu Yamamura of Tohoku University for his technical advice in electrochemical experiments. The authors wish to thank Mr. Roy Jacobus for his help in improving the understandability of the English expressions of this paper.

References

[1] A.N. Kamenskaya, Russ. J. Inorg. Chem. 29 (2) (1984) 251.
[2] L.B. Asprey, B.B. Cunningham, Prog. Inorg. Chem. 2 (1960) 267.
[3] D.A. Johnson, Adv. Inorg. Chem. Radiochem. 20 (1977) 1.
[4] L.J. Nugent, R.D. Baybarz, J.L. Burnett, J. Phys. Chem. 77 (12) (1973) 1528.
[5] A.N. Kamenskaya, N.B. Mikheev, N.P. Kholmogorova, Russ. J. Inorg. Chem. 28 (10) (1983) 1420.
[6] A.N. Kamenskaya, Dokl. Akad. Nauka SSSR 266 (2) (1982) 393 (in Russian).
[7] D.S. McClure, Z. Kiss, J. Chem. Phys. 39 (12) (1963) 3251.
[8] T. Nagai, T. Fujii, O. Shirai, H. Yamana, J. Nucl. Sci. Technol. 41 (6) (2004) 690.
[9] S.A. Kuznetsov, M. Gaune-Escard, Proceedings of the Workshop on Pyrochemical Separations, March 14–16, 2000, Avignon, France, 2000, pp. 295–305.
[10] T. Berzins, P. Delahay, J. Am. Chem. Soc. 75 (1953) 555.
[11] T. Fujii, H. Moiryama, H. Yamana, J. Alloys Compd. 351 (2003) L6.
[12] O. Terakado, S.Z. El Abedin, F. Endres, D. Nattland, W. Freyland, J. Non-Cryst. Solids 312–314 (2002) 459.
[13] K.E. Johnson, J.N. Sandoe, J. Chem. Soc. (A) (1969) 1695.